Corrugated composites: production-integrated quality assurance in carbon fiber reinforced thermoplastic sine wave beam production

Frederic J. C. Fischer, Matthias Beyrle, Arthur-Hans Thellmann, Manuel Endrass, Thomas Stefani, Tobias Gerngross, Michael Kupke

Angaben zur Veröffentlichung / Publication details:

Fischer, Frederic J. C., Matthias Beyrle, Arthur-Hans Thellmann, Manuel Endrass, Thomas Stefani, Tobias Gerngross, and Michael Kupke. 2017. "Corrugated composites: production-integrated quality assurance in carbon fiber reinforced thermoplastic sine wave beam production." *Advanced Manufacturing: Polymer & Composites Science* 3 (1): 10–20. https://doi.org/10.1080/20550340.2017.1283100.

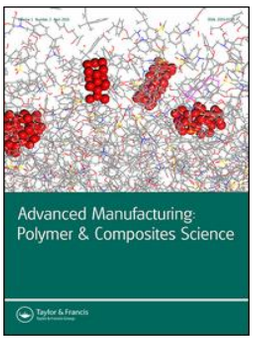

Taylor & Francis
Taylor & Francis Group

Advanced Manufacturing: Polymer & Composites Science

ISSN: 2055-0340 (Print) 2055-0359 (Online) Journal homepage: https://www.tandfonline.com/loi/yadm20

Corrugated composites: production-integrated quality assurance in carbon fiber reinforced thermoplastic sine wave beam production

Frederic J. C. Fischer, Matthias Beyrle, Arthur-Hans Thellmann, Manuel Endrass, Thomas Stefani, Tobias Gerngross & Michael Kupke

To cite this article: Frederic J. C. Fischer, Matthias Beyrle, Arthur-Hans Thellmann, Manuel Endrass, Thomas Stefani, Tobias Gerngross & Michael Kupke (2017) Corrugated composites: production-integrated quality assurance in carbon fiber reinforced thermoplastic sine wave beam production, Advanced Manufacturing: Polymer & Composites Science, 3:1, 10-20, DOI: 10.1080/20550340.2017.1283100

To link to this article: https://doi.org/10.1080/20550340.2017.1283100

Published online: 22 Feb 2017.

AMPCS Advanced Manufacturing: Polymer & Composites Science

Original Research Paper

Check for updates

Corrugated composites: production-integrated quality assurance in carbon fiber reinforced thermoplastic sine wave beam production

Frederic J. C. Fischer[1*], Matthias Beyrle[1], Arthur-Hans Thellmann[2], Manuel Endrass[1], Thomas Stefani[1], Tobias Gerngross[1], and Michael Kupke[1]

[1]Institute of Structures and Design (BT), Center for Lightweight Production Technology (ZLP), German Aerospace Center (DLR), Am Technologiezentrum 4, 86159 Augsburg, Germany
[2]Institute of Structures and Design (BT), Component Design and Manufacturing Technologies, German Aerospace Center (DLR), Pfaffenwaldring 38, 70569 Stuttgart, Germany

Abstract Carbon fiber-reinforced thermoplastics offer the possibility for short lead times and dustless assembly in aerospace applications. However, their great potential for efficient processing to date is not entirely exploited. At the Center for Lightweight Production Technology (ZLP) in Augsburg smart automation of thermoplastic composite production is investigated. To assess the overall process chain a sine wave beam designed as crash-absorber serves as demonstrator. The production process from as-delivered material to final assembly is presented. In addition to non-destructive testing at the end of the value adding process chain, production-integration quality assurance, and process characterization serve to evaluate each process step. In this context, water-coupled ultrasonic testing as an established method in aerospace production is used to assess the degree of consolidation after vacuum consolidation and press-forming. Thus, quality issues and crucial process parameters can be identified and optimized to improve robustness.

Keywords Carbon fiber-reinforced thermoplastics, Thermoplastic composites, Automation, Production technology, Vacuum consolidation, Thermoforming, Implant resistance welding, Production-integrated quality assurance

Cite this article Frederic J. C. Fischer, Matthias Beyrle, Arthur-Hans Thellmann, Manuel Endrass, Thomas Stefani, Tobias Gerngross and Michael Kupke: Adv. Manuf.: Polym. Compos. Sci., doi: 10.1080/20550340.2017.1283100

Introduction

Compared to aerospace grade thermosets the main advantages of carbon fiber-reinforced thermoplastic composites with matrices such as polyphenylene sulfide (PPS), polyetherimide (PEI), polyetherketoneketone (PEKK), and polyetheretherketone (PEEK) lies within the fact that these materials store at room temperature, allow faster cycle times by press forming, and dustless assembly by welding. Especially the field of joining and welding of thermoplastic composites has been studies extensively with a broad comprehensive knowledge base available.[1–10] Advanced manufacturing techniques have been discussed and demonstrated.[11–15] The so-called TAPAS (Thermoplastic Affordable Primary Aircraft Structure) consortium has demonstrated a number of large-scale thermoplastic components for aerospace applications since its launch in 2009.[16–18]

A high volume example of advanced thermoplastics usage in Aerospace is the use of thousands of clips and cleats within the structure of the A350 XWB. These clips are made of pre-consolidated laminate blanks,[19] often referred to as organo sheets. However, along this production route the design freedom in terms of prepreg material, layer orientation and local thickness variation is limited so that the potential of fiber-reinforced thermoplastics is not yet fully exploited.

At the DLR Center for Lightweight Production Technology (ZLP) research is focused on smart automation of carbon fiber-reinforced thermoplastic (CFRTP) production to push the technology readiness level (TRL) from demonstrator level which proves the general feasibility (TRL 3) to full-scale technology demonstration in an industry-like environment (TRL 6). For this purpose an automated process chain has been set up that allows swift adaptation to customization and product improvements.[20] Reproducible quality is ensured by means of production-integrated quality assurance. In this work, we have mainly focused on the degree of consolidation and the respective void content along the process chain which was identified as major issue in thermoplastic composite production.

Originally designed and validated as a crash-absorber for helicopter sub-floor configurations at the DLR Department for Structural Integrity[21,22] a sine wave beam serves to illustrate

*Corresponding author, email frederic.fischer@dlr.de

Received 21 September 2016 Accepted 25 December 2016
DOI 10.1080/20550340.2017.1283100

and assess the overall process capabilities from as delivered material to final part. The sine wave beam (see Fig. 1) is made of an upper and lower cap attached by two edge links to the sine wave web. The all-thermoplastic assembly is made of carbon fiber-reinforced polyetherimide (CF/PEI, TenCate Cetex® TC1000 Premium) material and joined by implant resistance welding. PEI film (SABIC ULTEM™ 1000) was used for the fabrication of pre-assembled resistance welding elements. The steel tooling for the complexly shaped edge links was designed to compensate spring-in effects.

Automated production

Figure 2 illustrates the established process chain at ZLP for thermoplastic CFRP parts. The process starts with the cutting of the prepreg material and ends with the joined assembly. The entire process chain with all its interfaces is investigated to identify optimization potentials.

For this purpose an integrated work cell has been set up to identify and assess viable technologies in an industry-oriented environment (see Fig. 3). In this cell an industrial robot for high temperature applications (KUKA KR210 R3100 Ultra F) is combined with a composite hot press system (WICKERT 4400 S). The hot press can be heated up to 450 °C at a platen size of 1800 mm by 1200 mm.

Thermoplastic preforming

Plies of thermoplastic prepregs are stacked and locally joined by ultrasonic spot welding. For this purpose a pick-and-place end effector is fitted with a special camera-based cut piece detection, as presented by Schuster *et al.*[23,24].

Process parameters for the ultrasonic spot welding of the prepreg plies with a 12 mm titanium stepped horn and a BRANSON 2000 LPe: 40:0.50.4T generator (40 kHz & 500 W) have been validated (Table 1). Spot welding with the 12 mm sonotrode shows no measurable effect on the organo sheet quality.[25] In addition, the web plies are only welded where the organo sheets are clamped during press processing and the final parts are trimmed.

Vacuum consolidation

Vacuum consolidation is an out of autoclave (OoA) vacuum bag technique especially suitable for pre-series and the manufacture of larger structures with smaller lot sizes like for instance stiffened fuselage skins or rudders.[26,27] In terms of design freedom it offers enhanced flexibility for parts and blanks of varying (local) thicknesses and adaptable build-up sequence of laminates since unique tooling is not required.

The welded laminate stacks are vacuum bagged and pre-consolidated at 310 to 320 °C in a hot air oven. The dwell time is roughly calculated with 10 min plus an additional minute per ply.[28] The maximum heating and cooling rates depend on the respective equipment (2–5 K/min). At ZLP we employ both a NABERTHERM N1500/45HA and a VÖTSCH VTU 300/300/500 circulating air oven for vacuum consolidation. The comparably small N1500/45HA (1 m × 1.5 m × 1 m) fulfils AMS 2750E requirements and reaches temperatures up to 450 °C. The VTU 300/500/300 (3 m × 5 m × 3 m) also meets aerospace demands for high temperature uniformity up to

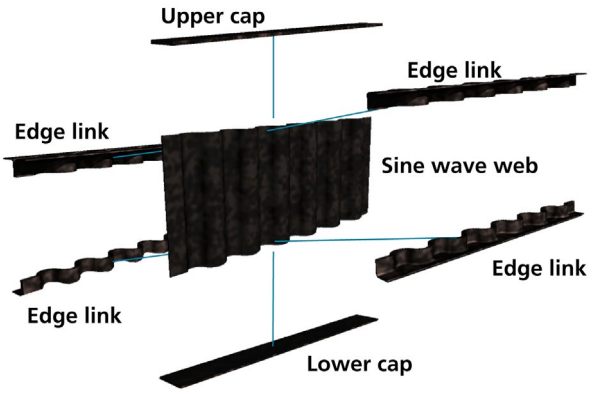

Figure 1 Thermoplastic composite process chain at ZLP

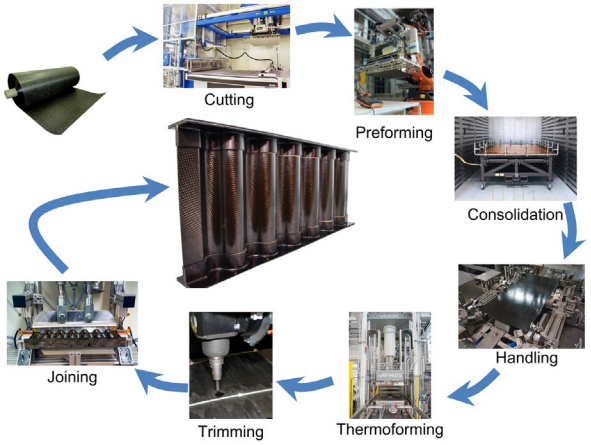

Figure 2 Sine wave beam components

Figure 3 Thermoplastic production cell at ZLP

Table 1 Weld processing window

Force	N	100–150
Pressure	MPa	1.0–1.2
On time	s	3
Hold time	s	2
Amplitude	µm	40–60

420 °C and allows the production of large thermoplastic structures. For the heat treatment in both furnaces special tooling equipment has been designed (see Figs. 4 and 5) with vacuum piping that is connected to rotary vane pumps.

Figure 6 shows a vacuum bag setup with its auxiliaries. The laminate stacks are placed between polyimide separation foils (UPILEX-125S) coated with release agent (MIKON® 705). The breather materials are based on desized glass fiber fabrics. If necessary, metal caul sheets atop the laminates can provide uniform surface finish. The outer polyimide vacuum foil is typically KAPTON 200HN fixed to the tooling with high temperature silicone sealant tape (AIRTECH A-800-3G or VBS 750).[29]

For enhanced process control the part temperatures are measured with thermocouples (type K) in between the upper, middle, and lower layers of preforms.

Organo sheet handling, preheating, and press forming

The press forming process is performed in combination of an infrared (IR) oven and a composite hot press (see Fig. 7).

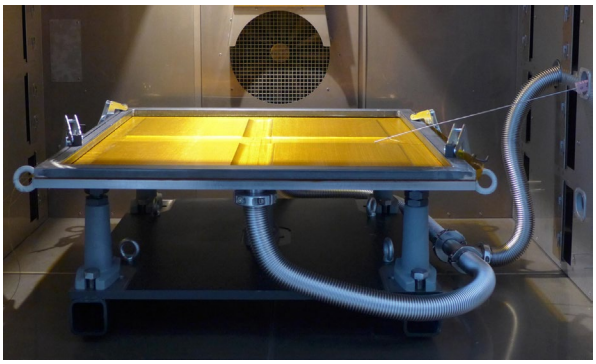

Figure 4 Transportable tooling (1 m × 1 m) for vacuum consolidation

Figure 5 Movable tooling (2 m × 3 m) for vacuum consolidation

In the IR-oven the organo sheets are rapidly heated above the melting temperature of the matrix (T_m(PEI) ~315 °C) at a rate of approximately 200 K/min. The top and bottom surface temperature are both measured by pyrometers and regulated individually. Depending on the number of layers the dwell time for a homogeneous temperature distribution within the organo sheet is set to 60 s for the edge links (with 6 layers) and 90 s for the sine wave web (with 8 layers). The distance between the IR-heater and the organo sheet is 100 mm on either side. The transfer time between the pre-heating stage up to the moment when pressure is applied was as short as 5.9 s. To ensure uniform pressure build-up the pressure is regulated by four plane-parallel cylinders.

Throughout the forming process the blanks are fixed in a clamping frame which sustains tension and keeps the blanks level once the softening temperature of the respective matrix system is reached (see Fig. 8). Thus, uniform heating without sagging is assured.

During press forming the softened blank is shaped following the tooling contour. The clamps at the outer corners of the frame then move along linear guides which allows for a defined and reproducible forming.

The clamping frame is activated automatically by a special docking station (see Fig. 9). Within this station the organo sheet is positioned and clamped prior to forming and afterward the respective final part is released herein.

Variothermic processing was carried out with the tool temperature set to 280 °C and an applied pressure of 15 MPa for 300 s, under consideration of the recommended processing window for compression molding of CF/PEI defined by Hou *et al.*[30,31] The parts were then cooled to 190 °C within the closed mold with the pressure still applied. Cooling time was approximately 20 min. These conditions were defined as benchmark.

For the alternative isothermal processing route the tool temperature was set to 190 °C, i.e. below the glass transition temperature of PEI (T_g ~ 215 °C). A processing window of pre-heating temperatures from 320 to 360 °C and applied pressures between 12.5 and 21 MPa was screened. The respective pressures were applied for 300 s.

Implant resistance welding

The assembly of the sine wave beam parts was carried out using implant resistance welding, a joining technique established for APC-2 PEEK Material by Freist[32] at the Institute of Structures and Design. The method was chosen following a thorough utility analysis[33] comparing thermoplastic joining methods[1,4,5,7,32,34–39] and adapted for the fiber-reinforced PEI matrix. The required process parameters namely electric power *P* and external joining force *F* were determined by a parametric scale up from specimen to demonstrator size.

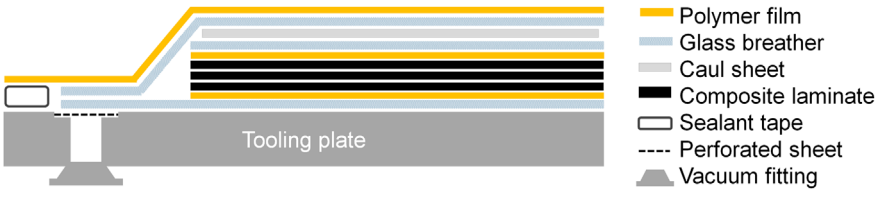

Figure 6 Vacuum bag setup for consolidation (Ref. [29])

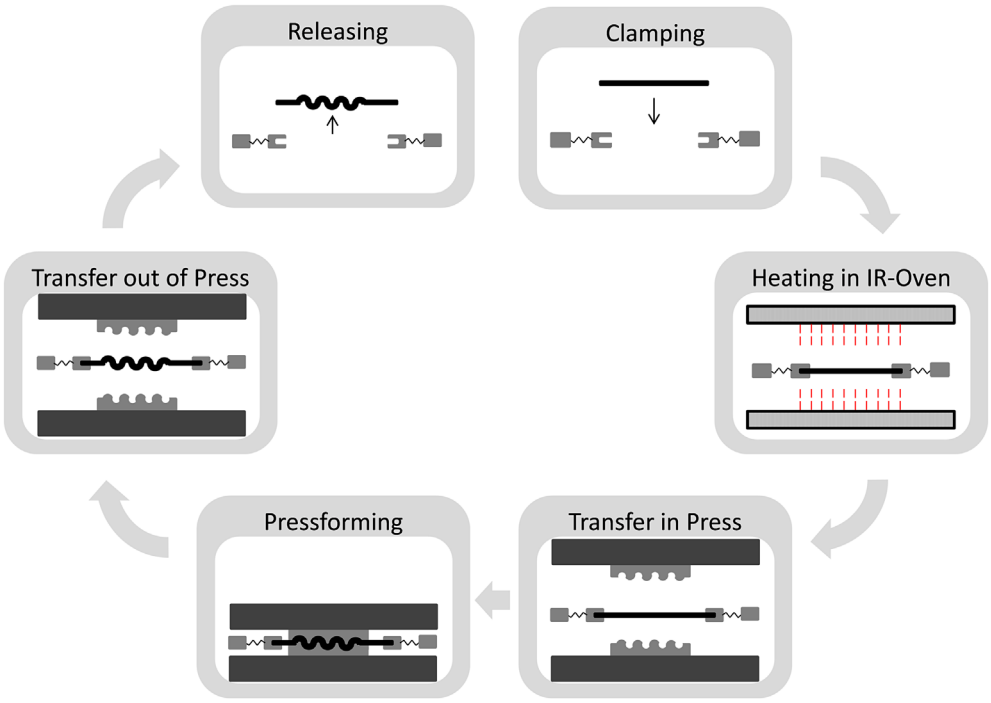

Figure 7 Diagram of the press forming process

Figure 8 Clamping frame in docking station before activation

Figure 9 Clamping frame with 3D part after press process

The electric power *P* depends on the geometrical dimensions of the weld element[1]:

$$P_{\text{nom}} = Pd \times w \times \left(L - \frac{4b}{3}\right)$$

where *Pd* represents the power density, *w* the width, *L* the length, and *b* the clamped length of the welding element.

The necessary joining force is calculated by multiplying the two-dimensional projected weld area $A_{\text{proj.}}$ by the maximum required pressure within the weld zone P_{max}:

$$F = P_{\text{max}} \times A_{\text{proj.}}$$

Before welding the mating surfaces were cleaned by sandblasting in order to remove potential impurities such as remains of release agent.

A 0.3 mm thick stainless steel mesh (ISO 1.4301) with a wire diameter of 0.065 mm was used as an electrical conductor. To prevent current leakage the mesh is sandwiched in between glass fiber polyetherimide semipregs with a 100 µm PEI film surface layer to form pre-assembled welding elements.

Copper clamps allow current flow through the stainless steel mesh which leads to the heating of the welding element and the adjacent joint area up to the melt temperature of the thermoplastic matrix (see Fig. 10). An electric power source provided 40 A of constant current output for 45 s.

An external force of 7.4 kN for the joining of the edge links to the web and 13.1 kN for the welding of the caps to the edge links was applied by two pneumatic cylinders to assure satisfactory consolidation. Due to the geometry of the corrugated web the resulting pressure on the inflection points is 30% lower compared to the upper/lower center points.

The setup of implant resistance welding of the edge link and the web is shown in Fig. 11, the final sine wave beam assembly in Fig. 12.

Production-integrated quality assurance

In general the goal of production-integrated quality assurance is to create a fundamental process understanding rather than relying on non-destructive testing of the final assembly. Within

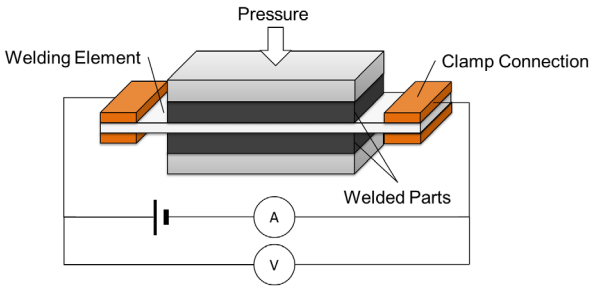

Figure 10 Schematic setup for the resistance welding process (adapted from Ref. [41] cited in Ref. [7])

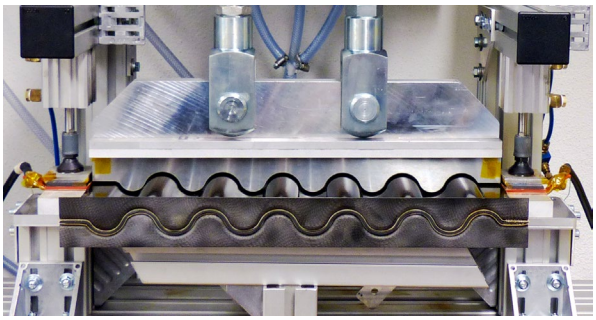

Figure 11 Experimental setup for the implant resistance welding of the sine wave beam parts

Figure 12 Final sine wave beam assembly

this scope production and part characterization is performed along the process chain.

For the part characterization water-coupled ultrasonic testing (WCUT) was carried out on the vacuum consolidated organo sheets and the variothermic press formed sine wave beam using the pulse-echo method. The test device was an Olympus OmniScan MX2 with a phased array module (OMNI-P-PA32:128), a 5MHz PA-probe with 64 elements (5L64-NW1), a wedge (SNW1) and a 2-axis encoding manual scanner (GLIDER 36 × 36).

In addition, thicknesses of the organo sheets and final parts were measured with a Kroeplin C450. The measurement tool has an accuracy of measurement of 0.02 mm.

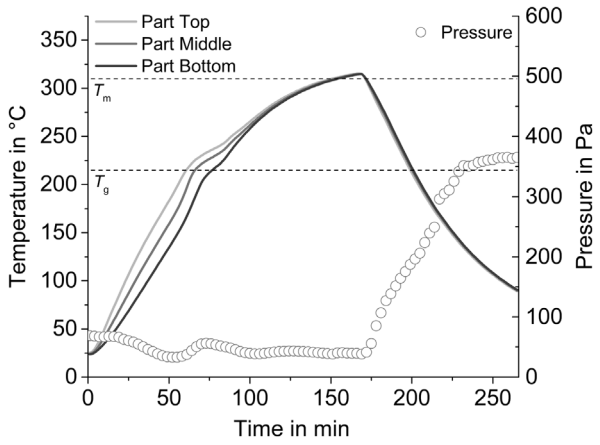

Figure 13 Temperature and pressure profile of a CF/PEI web laminate during vacuum consolidation in the furnace

The respective process data during vacuum consolidation and press forming were monitored and automatically stored.

Results

At DLR ZLP in Augsburg a process chain for the automated and flexible production of high performance thermoplastic composites combining vacuum consolidation and press forming was setup yielding CF/PEI parts, i.e. webs and edge links of good quality.

Pre-consolidated organo sheets

Figure 13 illustrates a temperature and pressure profile of a representative vacuum consolidation process. Once the glass transition temperature of the amorphous PEI matrix at about 215 °C is reached the temperature differences within the laminate stack (marked in gray) gradually reduce. The laminates remain at temperatures above 310 °C for 20 min according to the predefined heat treatment cycle. The pressure is measured at the inlet of the vacuum pump. During heating two minor peaks occur and pressure values increase up to 365 Pa (3.6 mbar) once the cooling sets in.

The movable tooling (see Fig. 5) was prepared for vacuum consolidation to produce 12 pre-consolidated blanks for webs and 8 blanks for the edge links. The blanks of the edge links were then water jet cut to form 24 single near net-shape blanks.

Organo sheets with thicknesses of 2.10 mm for the edge links and 2.80 mm for the web and excellent surface finish were produced. These values correspond to a consolidated thickness of 0.35 mm per ply. The thicknesses of the blanks slightly increase from the outer boundaries towards the center. For comparison commercial pre-consolidated organo sheets from TenCate show a consolidated thickness of 0.33 mm.

Water-coupled ultrasonic inspection of the consolidated blanks shows a comparably high amount of damping of the back-wall echo of the organo sheets. The gate was set over the estimated depth of the back-wall (2.5–4 mm). Figure 14(a) shows the A-, B-, C- and D-Scan of the amplitude data of an organo sheet with the A-Image at a spot in the middle of the organo sheet exactly at the intersection of the red lines in the C-Scan with low back-wall amplitude. The attenuation of the

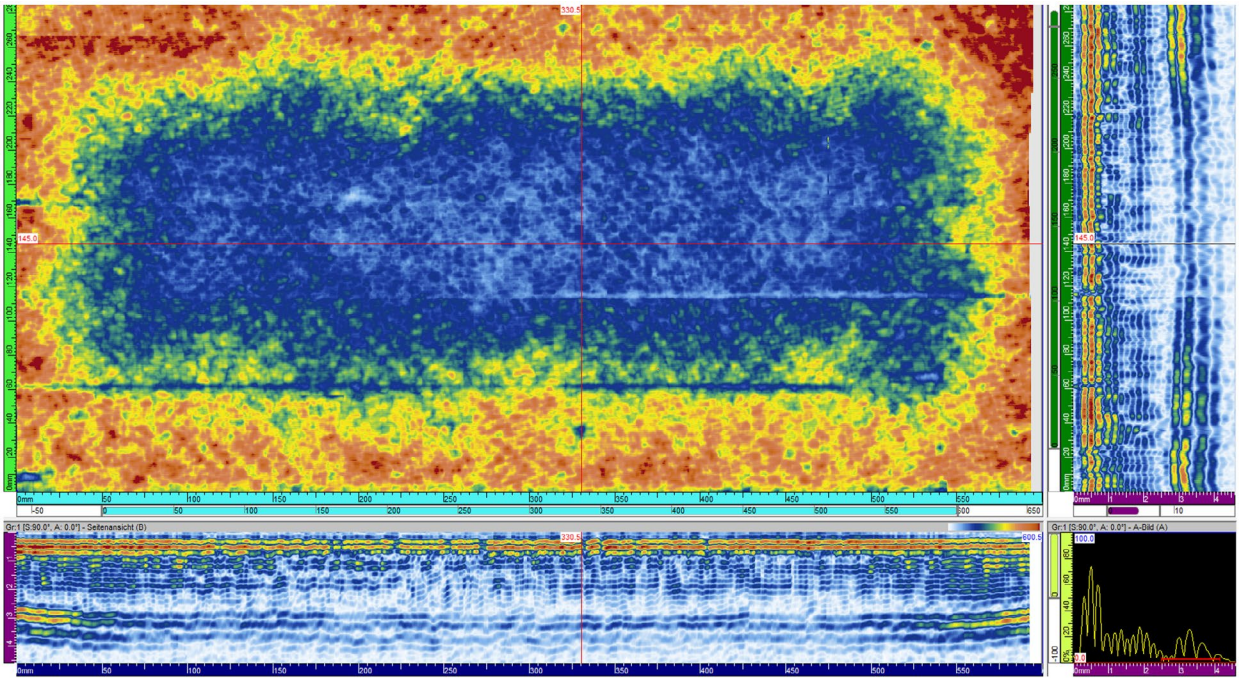

Figure 14a A-, B-, C-Scan and D-Scan of water-coupled ultrasonic testing of a web organo sheet

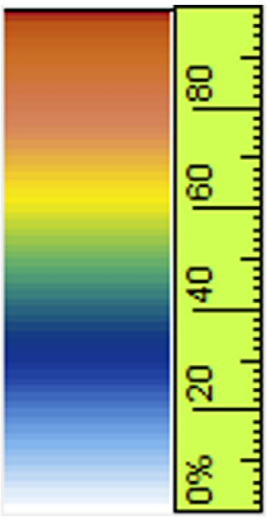

Figure 14b Colored scale of the ultrasonic amplitude level given in percentage

back-wall amplitude varies. Towards the outer edges of the rectangular blanks the amount of damping is gradually reduced (marked in yellow to red). According to the scale the colors from yellow to red correspond to a lower attenuation with an amplitude of the back-wall echo between 60 and 100% (see Fig. 14(b)).

The C-Scans of all produced organo sheets were projected on respective position of the blanks on the movable tooling (see Fig. 15). The blanks of the edge links (lowest row) show broader red edges indicating less back-wall attenuation compared to the web blanks.

Press formed webs

Compared to commercial organo sheets a reduced amount of swelling during the pre-heating in the IR-oven was observed with the in-house produced blanks.

The established variothermic processing renders molded parts with excellent surface quality (see Fig. 16) and an average thickness of 2.60 mm ± 0.13 mm (see Table 2). This thickness translates into a final consolidated thickness of 0.325 mm per ply, i.e. comparable to the commercial organo sheets.

For analysis and comparison the sine wave beam was subdivided into three regions (see Fig. 16). The plane regions at both ends (yellow), the hills and valleys (blue) and the inflection points (red).

Due to the geometry of the web no complete single C-Scan of the sine wave web was possible with the test equipment at hand. However, the flat flanks at the inflection points, as well as the upper region of the wave crest were successively tested. In order to maximize the investigated area the beam was scanned from both sides. Figure 17 shows the superposition of the sine wave beam with the resulting C-Image of the scan for one side of the beam.

The resulting A-, B-, C- and D-Scan of the bottom and top scan of the sine wave web are shown in Figs. 18 and 19, respectively. The gate for this evaluation was set over the estimated depth of the back-wall (2–3 mm).

The evaluation of the scan data shows a very high back-wall amplitude at the flat parts (approx. 100%) and a high amplitude at the top of the corrugated web (approx. 70%).

To examine the inflection point of the web a manual scan was performed without the 2-axis encoding scanner. The scan result (A- and B-Image) of one of these spots is shown in Fig. 20. The back-wall amplitudes at all measured spots was above 60%.

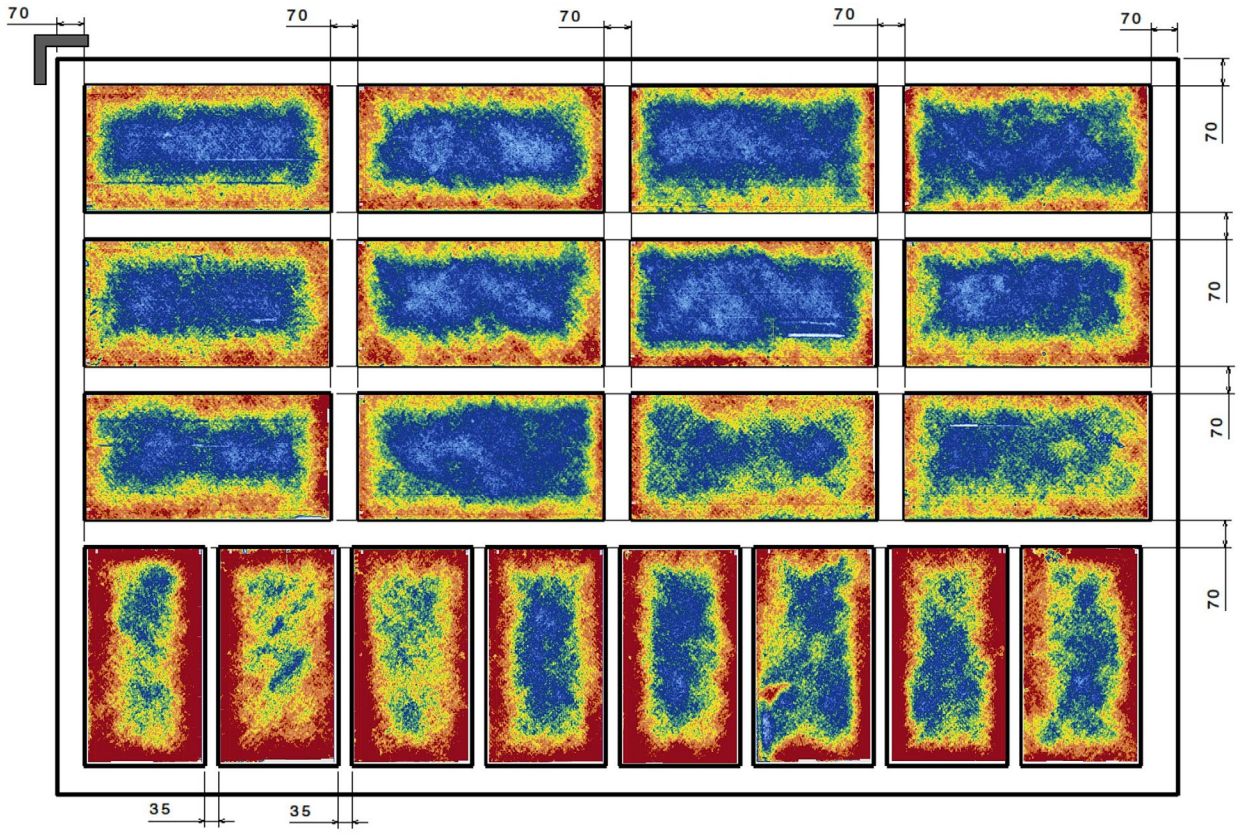

Figure 15 **WCUT C-Scans projected on the blank position on the movable tooling**

In addition, computed tomography (CT) was carried out on the aforementioned press molded (variothermic) web. Figure 21(a) shows the sectioned profile of the web with the plane region and the following two half cycles. Figure 21(b) illustrates the very same part region cut from atop thus showing the plane region and two inflection points. Figure 21(c) finally shows the hill of the second half cycle with its fiber orientation.

The thickness measurements illustrate perceivable differences along the distinct regions of the sine wave web and between the two processing routes (see Table 2). The thinnest areas are the plane regions, followed by the hills and valleys. The inflection points are thickest. No significant influence of the screened process parameters (IR-heating temperature and applied pressure) on the final thickness of the parts was found. Hence the average of all isothermally produced webs was calculated and compared to the variothermic benchmark. The thinnest isothermally formed web was produced at an IR temperature of 360 °C and an applied pressure of 18.8 MPa. Overall the isothermal webs are thicker than those formed by variothermic conditions. Besides, the surface of the specimen was slightly rougher.

Joined beam

In a first approach joining of the CF/PEI sine wave beam components by implant resistance welding could be successfully demonstrated. Minor wrinkle formation within the valleys of the corrugated edge links were observed.

Discussion

There is always an intrinsic amount of voids and enclosed gas in prepreg material. A certain amount of air is entrapped during the solvent impregnation process of the carbon fabric with PEI polymer which renders small bubbles on the surface of the prepreg. Voids exist within the fiber bundles, especially at the contact area between the warp and weft where impregnation is low since the polymer largely remains at the prepreg surface.[31]

These volatiles need to be removed during the manufacturing process since they may have detrimental effect on the parts mechanical properties. Therefore, for aerospace applications less than 1% void content must be achieved. The respective amount of acceptable back-wall attenuation is clearly defined in the AITM 6-4005.[40]

As for the results of ultrasonic testing the quality of pre-consolidated organo sheets would be regarded insufficient and thus rejected through standard non-destructive inspection. Due to the absence of a clear intermediate echo which would indicate flaws like delamination, big voids or layer porosity, the measured reduction of back-wall echo in WCUT is typically assigned to volume porosity.[40]

Since the thickness of the blanks was measured to be higher towards the center of the blanks one may expect a greater interply distance and possibly a higher amount of voids. Thickness was thus found to qualitatively correlate to the degree of consolidation of the organo sheets. Together

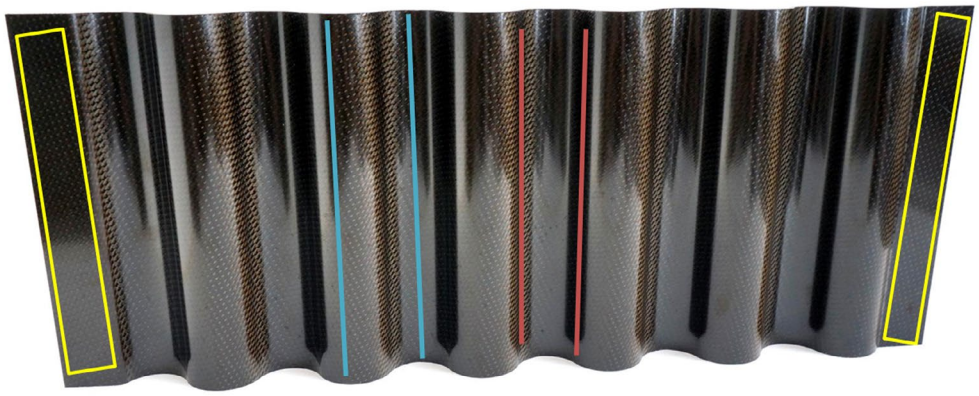

Figure 16 Variothermic produced sine wave web with marked regions for comparison

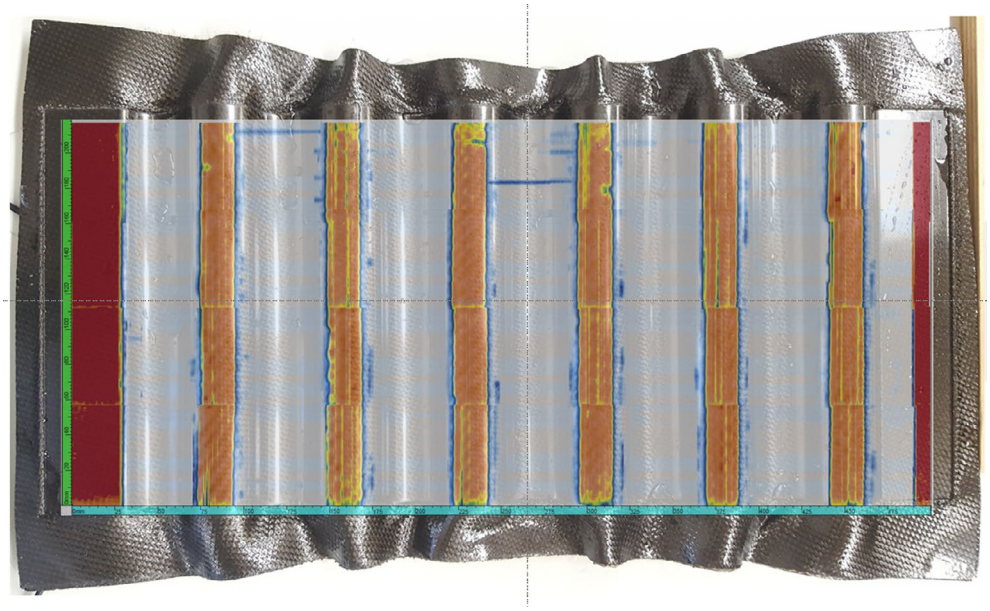

Figure 17 Superposition of the sine wave web and WCUT C-Scan data

Table 2 Average part thicknesses in variothermic and isothermal processing

	Plane region (mm)	Inflection point (mm)	Hill/valley (mm)	Total (mm)
Variotheric	2.40 ± 0.03	2.74 ± 0.05	2.52 ± 0.04	2.60 ± 0.13
Isothermal	2.68 ± 0.03	2.83 ± 0.04	2.72 ± 0.05	2.76 ± 0.07

with the results from the ultrasound inspection this hints at insufficient consolidation of the blanks. The fact that the thinner organo sheets of the edge links show less damping may hint at longer consolidation times or higher consolidation temperatures required.

Consolidation and void removal strongly depend on time, temperature and applied pressure during processing. In general, increasing either the applied pressure or the dwell time reduces the void content in the laminates, and thereby gives better consolidated composite parts.[30]

Hou *et al.*[30,31] suggested an impregnation model and defined a processing windows for successful compression molding of CF/PEI to reach void levels below 0.5%. Once T_g is reached the matrix melts and the entrapped air at the prepreg surface is removed. With the formation of resin-rich interlayers bonding of the single laminate layers is promoted. Once the layers are interconnected the wet out of fiber bundles takes place while the laminate is compacted due to the applied external pressure.

Consequently, vacuum consolidation for 20 min at 310 °C under atmospheric pressure (0.1 MPa) appears to be inappropriate to produce fully impregnated CF/PEI organo sheets. The impregnation model of Hou *et al.* suggest that a pressure of 2 MPa is required to provide a void content below 0.5%.[31] The remaining voids within the produced organo sheets are most likely not filled with compressed gas, since no swelling is observed during heating in the infrared furnace.

The comparison of the WCUT-scan data shows a significant increase of the back-wall amplitude between the pre-consolidated organo sheet and the press formed sine wave web. This amplification indicates sufficient consolidation after press forming. The different magnitudes between the measured back-wall amplitudes in the plane regions and the curved

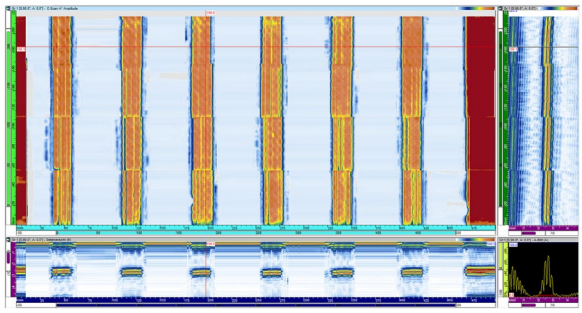

Figure 18 WCUT A-, B-, C- and D-Scan of the top of the sine wave web

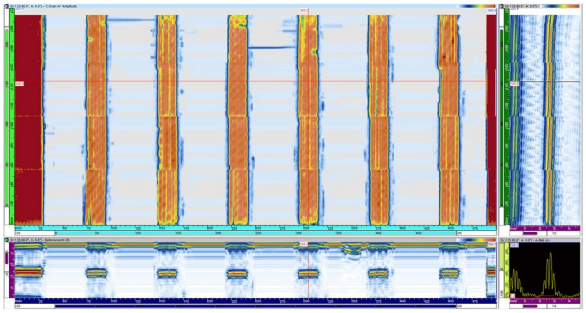

Figure 19 WCUT A-, B-, C- and D-Scan of the bottom of the sine wave web

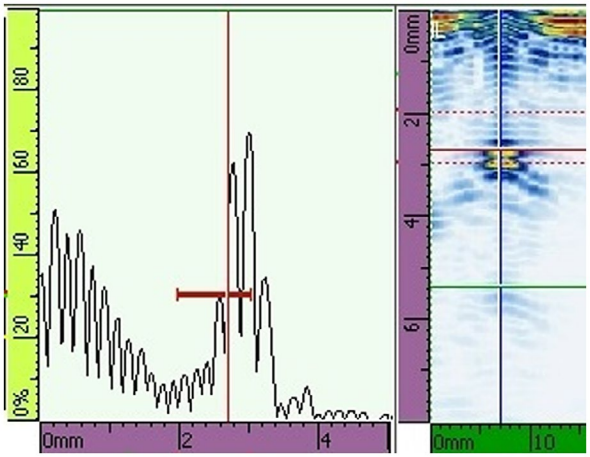

Figure 20 WCUT A- and B-Scan of a inflection point of the sine wave web

regions (see Figs. 17–19) may be attributed to difficult coupling and less reflection within the corrugated regions of the geometry.

In addition, computed tomography was carried out the sine wave web. The scans show a homogenously consolidated part with no traces of voids.

Concerning the web specimen produced isothermally the part quality in terms of thickness and surface quality could not meet the benchmark. However, the isothermal experiments have shown that with different process parameters similar part thicknesses are produced. Thus, we may state that the thermoforming process is comparably stable in terms of process deviations.

The tooling for the sine wave web has been constructed for an equal part thickness of 2.64 mm, i.e. consolidated ply thicknesses of 0.33 mm. This thickness is closely met by the webs that were produced by variothermic press forming. Thickness deviation at the inflection points could be assigned to fabrication tolerances of the tooling, where too much material was removed (approx. ±0.3 mm). In addition, due to the angle of 45° at the inflection points the resulting pressure is reduced by 30%.

The resulting thicknesses of the parts are primarily important when considering final assembly. With dimensional deviations arising from the tooling manufacture and those induced by the press forming process an overall mismatch between edge links and web parts is found. With the defined thickness of the pre-assembled welding elements, implant resistance welding technique is limited in terms of tolerance compensation. If pre-stressed parts are welded wrinkle formation may obviously occur to reduce the stresses. Ideally, these wrinkles may serve as trigger during crash loading.

Finally, destructive mechanical testing are yet to be performed to assess the overall part quality.

Conclusion and outlook

At the DLR Institute of Structures and Design an automated production of the sine wave beam assembly was realized. The obtained parts show good quality concerning surface finish after variothermic press forming. Production processes for CF/PEI organo sheets and press molded parts have been established. Production-integrated quality assurance was mainly based on aerospace standard water-coupled ultrasonic testing to assess the degree of consolidation throughout the process. Together with the monitored processing data and measured part thicknesses a sound process understanding was established.

Tooling infrastructure, vacuum setup and heating cycles for the vacuum consolidation of CF/PEI and other high performance thermoplastics in the furnace have been established and probed. Only pre-consolidation of the preformed ply stacks was achievable and higher consolidation pressures appear to be required.

Vacuum consolidation due to its high flexibility may still be considered a viable technique, however, limited to certain prepreg materials. Pre-consolidation of CF/PEI prepregs in a vacuum process reduces the amount of gas inclusions between the stacked plies, which might else hinder through thickness heating in the IR-furnace and support delamination during thermoforming.

The established variothermic press processing, including clamping, preheating and press forming has produced parts with reproducible dimensions and excellent surface finish. The goal of a thermoforming process at constant mold temperature avoiding cyclic heating and cooling to significantly reduce the process time was achieved, however, leading to declined surface quality of the produced parts.

The sine wave beam was successfully joined by implant resistance welding. The observed wrinkle formation after welding is most likely caused by dimensional deviations between edge link and web. These will be removed by adaptions to the tooling after design iteration within our closed-loop setup in

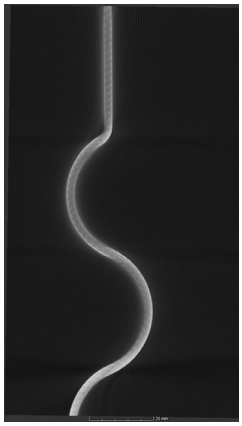

Figure 21a CT cross section profile of the sine wave web

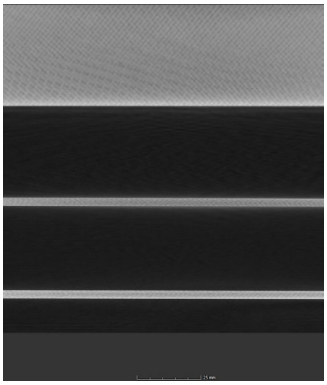

Figure 21b CT plan view section of the sine wave web

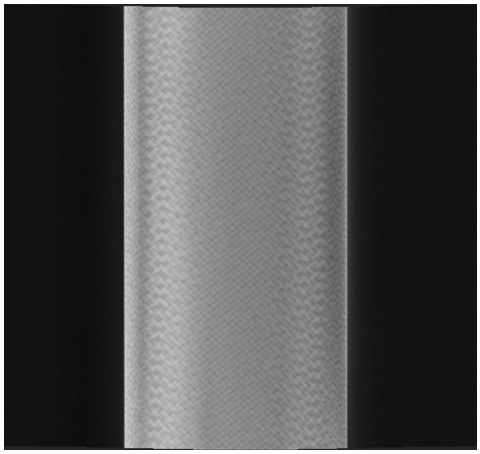

Figure 21c CT scan of a hill of the sine wave web

the Institute of Structures and Design. Tolerance management remains a crucial issue that needs to be considered for every assembly.

With the setup and trial of a full-scale ready process chain substantial expertise in the field of production technology was gathered which now serves as a basis for future optimization and enhancements. Production-integrated quality assurance was found to be essential for the overall process assessment.

Acknowledgments

Special thanks goes to all the other members of the project team at the Institute of Structures and Design in Augsburg and Stuttgart namely Georg Braun, Georg Doll, Manuel Engelschall, Philipp Gänswürger, Roland Glück, Raouf Jemmali, Leonhard Häberle, Michael Kühnel, Mario Sabino Cozzolino, Manfred Schönheits, Alfons Schuster and Fabian Zimmermann for their contributions in this DLR funded project. Moreover we would like to express our gratitude to Mr. Olaf Sirges at SABIC Innovative Plastics GmbH for his support and expertise on ULTEM™ 1000 PEI film.

Disclosure statement

No potential conflict of interest was reported by the authors.

Funding

Research funded by Deutsches Zentrum für Luft- und Raumfahrt.

ORCID

Frederic J. C. Fischer http://orcid.org/0000-0001-5421-4336
Matthias Beyrle http://orcid.org/0000-0002-3164-1068
Manuel Endrass http://orcid.org/0000-0003-4133-0834

References

1. C. Ageorges and L. Ye: 'Fusion bonding of polymer composites: from basic mechanisms to process optimisation', 1st edn, (ed. P. B. Derby), 2002, London, Springer-Verlag. Available from: http://dx.doi.org/10.1007/978-1-4471-0171-0.
2. C. Ageorges, L. Ye and M. Hou: 'Advances in fusion bonding techniques for joining thermoplastic matrix composites: a review', Composites Part A: Applied Science and Manufacturing. 2001, **32**, 839–857. Available from: http://dx.doi.org/10.1016/S1359-835X(00)00166-4.
3. A. Benatar and T. G. Gutowski: 'Methods for fusion bonding thermoplastic composites', *Composites*. Elsevier BV; 1986, **18**, 35–42. Available from: http://dx.doi.org/10.1016/0010-4361(88)90606-4.
4. D. A. Grewell, A. Benatar and J. B. Park: 'Plastics and composites welding handbook', 2003, Munich, Hanser Gardener.
5. L. Moser, I. F. Villegas, P. Mitschang, H. Bersee and A. Yousefpour: 'Comparison of three welding processes for joining advanced thermoplastic composites', Int. SAMPE Symposium and Exhibition (Proceedings), Seattle, WA, 2010. Available from: http://www.scopus.com/inward/record.url?eid=2-s2.0-78649465330&partnerID=40&md5=1b6dc32e5f65ba06c9041d7bd53f35f9.
6. F. Senders, M. van Beurden, G. Palardy and I. F. Villegas: 'Zero-flow: a novel approach to continuous ultrasonic welding of CF/PPS thermoplastic composite plates', Advanced Manufacturing: Polymer & Composites Science. Taylor & Francis; 2016, **2**, 83–92. Available from: http://dx.doi.org/10.1080/20550340.2016.1253968.
7. D. Stavrov and H. E. N. Bersee: 'Resistance welding of thermoplastic composites-an overview', *Composites Part A: Applied Science and Manufacturing*, Elsevier BV; 2005, **36**, 39–54. Available from: http://dx.doi.org/10.1016/S1359-835X(04)00182-4.
8. I. F. Villegas and H. E. N. Bersee: 'Ultrasonic welding of advanced thermoplastic composites: an investigation on energy-directing surfaces', *Adv. Polym. Tech.*, Wiley-Blackwell; 2010, **29**, 112–121. Available from: http://dx.doi.org/10.1002/adv.20178.
9. I.F. Villegas, L. Moser, A. Yousefpour, P. Mitschang and H. E. Bersee: 'Process and performance evaluation of ultrasonic, induction and resistance welding of advanced thermoplastic composites', J. Thermoplast. Compos. Mater., Sage; 2012, **26**, 1007–1024. Available from: http://dx.doi.org/10.1177/0892705712456031.
10. R. Rudolf, P. Mitschang and M. Neitzel: 'Induction heating of continuous carbon-fibre-reinforced thermoplastics', Composites Part A: Applied

Science and Manufacturing, Elsevier BV; 2000, **31**, 1191–1202. Available from: http://dx.doi.org/10.1016/S1359-835X(00)00094-4.
11. U. P. Breuer: 'Beitrag zur Umformtechnik gewebeverstärkter Thermoplaste [A contribution to the forming technology of fabric-reinforced thermoplastic composites]', 1997, Düsseldorf, Technische Universität Kaiserslautern. Available from: http://d-nb.info/951333968.
12. M. Christmann, L. Medina and P. Mitschang: 'Effect of inhomogeneous temperature distribution on the impregnation process of the continuous compression molding technology', *J. Therm. Compos. Mater.*, Sage; 2016. Available from: http://dx.doi.org/10.1177/0892705716632855.
13. J. Nowacki and M. Neitzel: 'Thermoforming of reinforced thermoplastic stiffened structure', *Polym. Compos.*, Wiley; 2000, **21**, 531–538. Available from: http://dx.doi.org/10.1002/pc.10208.
14. T. Lafuente, J. Nowacki, P. Mitschang, A. T. Marques and M. Neitzel: 'Tailored blank technology: a one-step-process', *J. Therm. Compos. Mater.* Sage; 2002, **15**, 355–371. Available from: http://dx.doi.org/10.1177/089270502015004734.
15. F. C. Campbell: 'Thermoplastic composites: an unfulfilled promise', Chap. 10, in 'Manufacturing processes for advanced composites', (ed. F. C. Campbell), 357–397; 2004, Amsterdam, Elsevier Science. Available from: http://dx.doi.org/10.1016/B978-185617415-2/50011-3.
16. G. Gardiner: 'Thermoplastic composites: primary structures?', *High-Performance Compos*. 2011, **19**, 52–59. Available from: http://www.compositesworld.com/articles/thermoplastic-composites-primary-structure.
17. A. Offringa: 'New thermoplastic composite design concepts and their automated manufacture', *JEC Compos. Mag*. 2010, 45–49. Available from: http://www.jeccomposites.com/news/composites-news/new-thermoplastic-composite-design-concepts-and-their-automated-manufacture.
18. J. Sloan: 'TAPAS 2: next steps in thermoplastic aerostructures', 2014. Available from: http://www.compositesworld.com/articles/tapas-2-next-steps-in-thermoplastic-aerostructures.
19. K. Edelmann, A. Miaris, M. Ulrich, T. Neitzel and T. Frese: 'Thermoplastische Bauteile entstehen im Minutentakt', Fachtagung Carbon Composites Kongresszentrum Augsburg: Vogel Business Media; 2014. Available from: http://www.fachtagung-carboncomposites.de/de/reviews/#vortraege.
20. F. J. C. Fischer, M. Beyrle, M. Endraß, L. Häberle, T. Stefani, G. Matthias, P. Gänswürger, G. Braun, and M. Kupke: 'Automated production of carbon fiber reinforced thermoplastic sine wave beams', Proc. 17th Eur. Conf. on 'Composite Materials ECCM 17', Munich, Germany, 2016.
21. C. M. Kindervater and H. Georgi: 'Composite strength and energy absorption as an aspect of structural crash resistance', in 'Structural crashworthiness and failure, (ed. N. Jones and T. Wierzbicki), 162–203; 1993, London, Taylor & Francis.
22. D. Kohlgrueber: 'Validation of a frabric model for crash simulations of composite structures', '24th SAMPE Europe', Paris, France, 2003, 413–422.
23. M. Kühnel, A. Schuster, C. Rähtz and M. Kupke: 'Tailored thermoplastic preforming with continuously automated cutting and robotic pick and place processes of various semi-finished goods', Proc. 17th Eur. Conf. on 'Composite Materials ECCM 17', Munich, Germany, 2016.
24. A. Schuster, M. Kühnel and M. Kupke: 'Automated preforming of curved thermoplastic organic sheets', 'SAMPE Europe Conference', Amiens, SAMPE, 2015.
25. Y. Mezakeu Tongnan and F. J. C. Fischer: 'Untersuchung zum Einfluss von Ultraschallheftstellen beim Preforming auf die Organoblechqualität carbonfaserverstärkter Hochleistungsthermoplaste [Investigation on the influence of ultrasonic welding during preforming on the organo sheet quality of carbon fiber-reinforced high performance thermoplastics]', Report No.: DLR-IB-BT-AU-2016-75, Deutsches Zentrum für Luft- und Raumfahrt (DLR), Augsburg, 2016, 80. Available from: http://elib.dlr.de/104094/
26. AVK - Industrievereinigung Verstärkte Kunststoffe e.V: 'Handbuch Faserverbundkunststoffe – Grundlagen, Verarbeitung, Anwendungen', (ed. Witten, E), 311–542; 2010, Wiesbaden, Springer Nature Vieweg + Teubner.
27. G. Kempe and L. Häberle: 'Vacuum consolidation technique as a cost effective manufacturing technology for continuous fibre reinforced thermoplastics', Int. Workshop on 'Thermoplastic Matrix Composites', Gallipoli, 2003.
28. G. Kempe: 'Duroplastische und Thermoplastische Faserverbundwerk stoffe–Vorteile–Eigenschaften–Verarbeitung und Anwendungsgebiete beider Werkstoffgruppen', in 'Faserverbundwerkstoffe mit thermo-plastischer Matrix, (ed. W. J. Bartz and E. Wippler), 44–74; 1997, Renningen, Expert-Verlag.
29. F. Fischer, Y. Mezakeu Tongnan, M. Beyrle, T. Gerngross and M. Kupke: 'Characterization of production-induced defects in carbon fiber reinforced thermoplastic technology', 7th Int. Symp. on 'NDT in Aerospace', DGZfP, FhG, Bremen, 2015. Available from: http://www.ndt.net/article/aero2015/papers/tu1a2.pdf.
30. M. Hou, L. Ye, H. Lee and Y. Mai: 'Manufacture of a carbon-fabric-reinforced polyetherimide (CF/PEI) composite material', Compos. Sci. Technol., Elsevier BV; 1998, **58**, 181–190. Available from: http://dx.doi.org/10.1016/S0266-3538(97)00117-6.
31. M. Hou, L. Ye and Y. W. Mai: 'Manufacturing process and mechanical properties of thermoplastic composite components', J. Mater. Process. Technol., Elsevier BV; 1997, **63**, 334–338. Available from: http://dx.doi.org/10.1016/s0924-0136(96)02644-1.
32. C. Freist: 'Experimentelle und numerische Untersuchungen zum Widerstandsschweißen endlosfaser- und kurzfaserverstärkter thermoplastischer Hochleistungsstrukturen [Experimental and numerical analysis of the resistance welding of continuous and short fiber reinforced thermoplastic structures]', Universität Stuttgart, Stuttgart, 2013. Available from: http://dx.doi.org/10.18419/opus-3918.
33. M. Endraß and L. Häberle: 'Jahresabschlussbericht 2015 Protec Wellholm – AP15 Fügen der Bauteile [Annual report 2015 Protec Wellholm - AP15 joining of components]', Report No.: DLR-IB-BT-AU-2016-74, Deutsches Zentrum für Luft- und Raumfahrt (DLR), Augsburg, 2016. Available from: http://elib.dlr.de/103917/
34. M. Arias: 'Experimentelle Untersuchung des kontinuierlichen und gepulsten Widerstandsschweißen als Fügeverfahren zur Herstellung von Faserverbundbauteilen mit thermoplastischer Matrix [Experimental investigation on continuous and pulsed resistance welding as a joining method for the manufacture of fiber-reinforced parts with thermoplastic matrix]', ETH Zürich, Zürich, 1998. Available from: http://dx.doi.org/10.3929/ethz-a-001988460.
35. M. Dubé, P. Hubert, A. Yousefpour, and J. Denault: 'Current leakage prevention in resistance welding of carbon fibre reinforced thermoplastics', *Compos. Sci. Technol.*, Elsevier BV; 2008, 68, 1579–1587. Available from: http://dx.doi.org/10.1016/j.compscitech.2007.09.008.
36. M. Hou, L. Ye and Y.-W. Mai: 'An experimental study of resistance welding of carbon fibre fabric reinforced polyetherimide (CF Fabric/PEI) composite material. *Appl. Compos. Mater.*. Springer Nature; 1999, **6**, 35–49. Available from: http://dx.doi.org/10.1023/A:1008879402267.
37. G. Kempe and L. Häberle: 'Fügetechniken für endlosfaserverstärkte Thermoplaste. Internationale Konferenz Schweisstechnik, Werkstoffe und Werkstoffprüfung, Bruchmechanik und Qualitätsmanagement'. Vienna; 1997, 659–668. Available from: https://www.tib.eu/en/search/id/tema%3ATEMAM98022338560/F%C3%BCgetechniken-f%C3%BCr-endlosfaserverst%C3%A4rkte-Thermoplaste/?tx_tibsearch_search%5Bsearchspace%5D=tn.
38. L. Häberle: 'Workshop Fügetechnik "Direktfügen" Verfahrensübersicht', Deutsches Zentrum für Luft- und Raumfahrt (DLR); Stuttgart, 2009.
39. L. Häberle: Widerstandsschweißen mit VA-Mesh. Report No. DLR-IB 435–2009/43. Deutsches Zentrum für Luft- und Raumfahrt (DLR), Stuttgart, 2015. Available from: http://elib.dlr.de/61035/.
40. AIRBUS: 'Airbus Test Method For Inspection Processes AITM6-4005: ultrasonic pulse-echo inspection of carbon fibre plastics', Blagnac, 2011.
41. D. Stavrov and H. E. N. Bersee: 'Thermal aspects in resistance welding of thermoplastic composites', Proc. 'ASME Summer Heat Transfer Conference', Las Vegas, NV, ASME International, 2003, 151–156.